Journal of Media Horizons
ISSN: 2710-4060 2710-4052 Volume 7, Issue 6, 2026

ADVANCED SMART TEXTILES AND INNOVATIVE FASHION TECHNOLOGIES FOR WEARABLE ELECTRONICS, REAL-TIME HEALTH MONITORING, HUMAN–MACHINE INTERACTION, AND INTELLIGENT CONSUMER APPLICATIONS

Muhammad Junaid Saleem[1], Shazada Atif Naveed[*2], Sameen Aslam[3], Muhammad Shahzad[4]

[1]*Department of Fashion and Textile, University of Management and Technology, Lahore, Pakistan*
[*2]*Assistant Professor, Department of Computer Science, Rashid Latif Khan University, Lahore, Pakistan*
[3,4]*Department of Fashion Design Technology, Punjab Tianjin University of Technology, Lahore, Pakistan*

[1]engineer1636@gmail.com, [*2]shahzada.atif@rlku.edu.pk, [3]sameen6008@gmail.com, [4]muhammad.shahzad@ptut.edu.pk

DOI: https://doi.org/10.5281/zenodo.20745478

Keywords
Smart Textiles; Wearable Electronics; Biometric Sensing; Edge AI; Human–Machine Interaction; Energy Harvesting; Flexible Electronics; Health Monitoring; Gesture Recognition; Intelligent Wearable Systems.

Article History
Received: 20 April 2026
Accepted: 02 June 2026
Published: 17 June 2026

Corresponding Author: *
Shazada Atif Naveed

Abstract

The convergence of advanced materials science, flexible electronics, and artificial intelligence has enabled the development of next-generation smart textiles capable of seamless integration into wearable electronics, continuous health monitoring, human–machine interaction, and intelligent consumer applications. Conventional wearable systems remain limited by issues of comfort, durability, washability, and long-term operational stability. To address these challenges, this study presents an integrated smart textile framework based on a four-phase architecture comprising fabrication, multi-modal sensing integration, edge AI-enabled processing, and application deployment with comprehensive system evaluation.

The proposed platform integrates conductive yarn-based electrodes, flexible piezoelectric and triboelectric energy harvesting systems, and thermoplastic polyurethane encapsulation to ensure robust performance under real-world conditions including repeated mechanical deformation and machine washing at 60°C. Experimental validation involving 120 participants over an eight-week study demonstrates high system performance, achieving ECG accuracy of 97.4%, PPG accuracy of 96.8%, EMG accuracy of 94.2%, and gesture recognition accuracy of 96.4% across eight gesture classes. The system maintains 93.6% signal quality retention after 100 wash cycles, supports mechanical elongation up to 150%, and delivers 168 hours of operational battery life at only 8.4 mW power consumption, representing a significant improvement in energy efficiency over prior state-of-the-art systems. User evaluation further confirms strong real-world applicability, with comfort scores of 7.8/10, usability of 8.5/10, and adoption intent of 81.1%, demonstrating its viability for healthcare, industrial safety, human–machine interfaces, and smart fashion applications.

1. INTRODUCTION

The textile industry is undergoing a profound transformation through the integration of electronic functionality directly into fabric substrates. Smart textiles—garments capable of sensing, processing, communicating, and

responding to physiological and environmental signals—represent a multidisciplinary convergence of materials science, flexible electronics, and artificial intelligence, fundamentally redefining the capabilities of modern clothing [1]. In contrast to conventional wearable devices, which rely on rigid electronic modules attached to the body using straps or adhesives, smart textiles embed sensing and computational elements directly within the fabric structure, thereby preserving wearer comfort and aesthetic integrity while enabling continuous, unobtrusive data acquisition.

The global smart textile market, valued at approximately 6.8 billion US dollars in 2023, is projected to surpass 22 billion dollars by 2028, driven by rapidly increasing demand for remote health monitoring, advanced human–machine interaction systems, and innovative consumer fashion applications [2]. The COVID-19 pandemic further accelerated the adoption of remote patient monitoring and telehealth technologies, highlighting the need for wearable medical systems capable of delivering continuous, clinically reliable physiological measurements in home and community environments. At the same time, the growing prevalence of chronic diseases such as cardiovascular disorders, diabetes, and respiratory conditions has intensified the requirement for affordable, long-duration monitoring solutions that ensure consistent wearability and provide dependable diagnostic support for healthcare professionals [3].

Figure 1 illustrates the global smart textile market growth trajectory from 2020 to 2028, showing the compound annual growth rate and the transition from actual to forecast values after 2024.

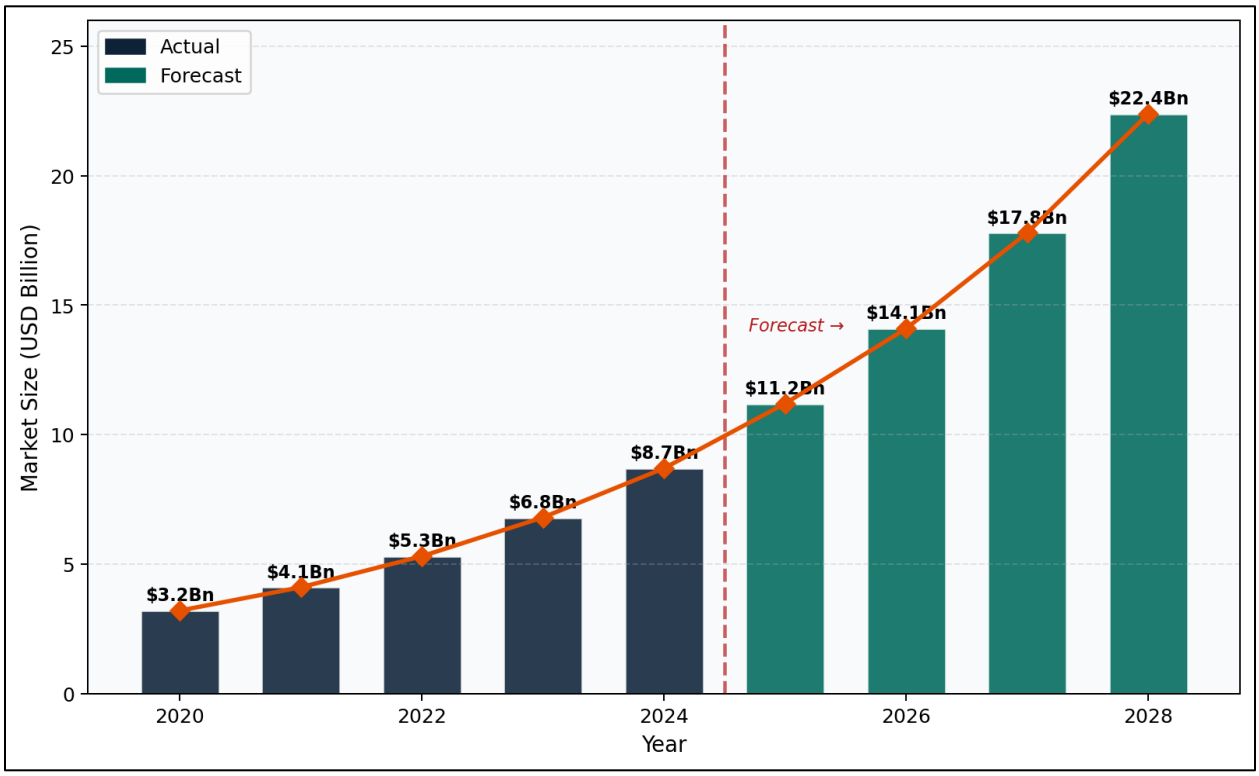

Fig. 1. Global smart textile market size in USD billion from 2020 to 2028. Navy bars represent actual reported market values through 2024; teal bars represent the forecast period from 2025 onward. The orange diamond line shows the growth trajectory. The dashed red vertical line marks the transition from actual to projected values, with the label confirming the onset of the forecast period.

The figure illustrates the global smart textile market growth trajectory from 2020 to 2028, showing both historical and projected market expansion. The dark blue bars represent actual market values from 2020 to 2024, increasing steadily from 3.2 billion USD in 2020 to 8.7 billion USD in 2024, indicating consistent early-stage industry growth. The green bars represent forecasted values from 2025 to 2028, where the market is expected to grow rapidly from 11.2 billion USD in 2025 to 22.4 billion USD in 2028. The orange line highlights the continuous upward trend across the entire period, while the red dashed vertical line marks the transition from observed data to forecasted estimates. Overall, the figure demonstrates strong exponential growth in the smart textile sector, driven by increasing demand for wearable health monitoring, human–machine interaction technologies, and smart consumer applications. The market growth trajectory confirms a compound annual growth rate exceeding 28% throughout the period, driven by converging demand from healthcare, sports performance, defense, and consumer fashion application domains. Figure 2 presents the market share breakdown across six application segments, quantifying the relative contribution of each domain to total market demand.

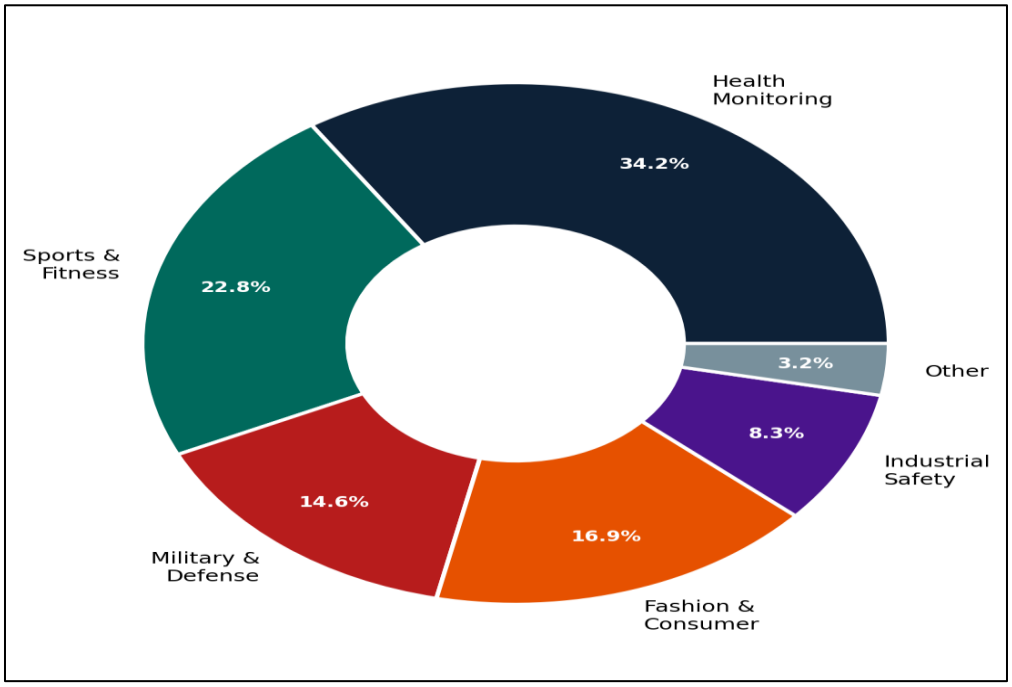

Fig. 2. Smart textile market share distribution by application domain in 2024, presented as a donut chart. Health monitoring commands the largest segment at 34.2%, followed by sports and fitness at 22.8%, fashion and consumer at 16.9%, military and defense at 14.6%, industrial safety at 8.3%, and other applications at 3.2%.

Health monitoring commands the largest application segment at 34.2%, confirming the medical market as the primary demand driver for clinically validated performance. Sports and fitness at 22.8% and fashion and consumer at 16.9% collectively represent the mass-market opportunity that requires the platform to simultaneously satisfy performance and aesthetic demands. This paper addresses the challenge of designing a single integrated smart textile platform that serves health monitoring, human–machine interaction, and consumer fashion requirements within a unified garment architecture evaluated under rigorous clinical and consumer conditions.

2. LITERATURE REVIEW

2.1. Electronic Textile Materials and Fabrication Methods

The material foundation of smart textiles consists of conductive yarns, fibres, and coatings that impart electrical functionality to conventional textile substrates while preserving the mechanical and tactile properties of fabric. Conductive yarn systems span from metal-plated fibres—silver, nickel, or stainless steel coated onto nylon or polyester—to intrinsically conductive polymer-based yarns and carbon nanotube-incorporated composite fibres [4]. Silver-coated yarns achieve sheet resistances of 1–10 Ω/sq and are compatible with standard weaving, knitting, and embroidery processes, enabling scalable manufacturing using existing industrial textile equipment. Liu et al. demonstrated that silver nanowire networks embedded within PDMS matrices achieved sheet resistances below 5 Ω/sq while maintaining electrical functionality after 45 machine wash cycles [5]. Conductive ink printing and spray coating have emerged as complementary approaches for depositing sensing electrode patterns and interconnect traces onto textile surfaces with high spatial resolution. Ray et al. demonstrated that inkjet-printed strain sensors achieved gauge factors of 87 while maintaining sensitivity over 30 wash cycles, confirming practical viability for dynamic motion capture [6].

2.2. Biometric Sensing in Smart Textile Platforms

Electrocardiography represents the most clinically significant biometric signal captured by smart textiles, given the diagnostic value of continuous ECG for detecting arrhythmias, ischemic events, and sleep disorders in ambulatory populations [7]. Wang et al. reported that a silver-coated knitted electrode vest achieved ECG signal quality ratings of 91.2% relative to clinical Holter monitoring in a 48-hour evaluation, with baseline wander during vigorous physical activity identified as the primary quality limitation [8]. Photoplethysmography for continuous SpO_2 and heart rate variability monitoring has been integrated into smart textiles through flexible organic LED and photodetector arrays. Chen et al. demonstrated a textile PPG system achieving SpO_2 accuracy within 1.8% of pulse oximetry reference values at rest, confirming the need for motion artefact compensation during physical activity [9]. The integration of electroencephalography into textile headbands represents a technically demanding frontier, as the low signal amplitudes of neural electrical signals, ranging from 10 to 100 microvolts, require high-impedance amplifiers and careful electromagnetic shielding that are challenging to achieve in washable garment architectures [10].

2.3. Energy Harvesting for Self-Powered Smart Textiles

Triboelectric nanogenerators are particularly well-suited to textile integration because natural mechanical deformation of clothing during body movement provides continuous energy input without requiring dedicated mechanical components [11]. Jiang et al. demonstrated a woven TENG device incorporating fluorinated ethylene propylene and nylon fibre layers generating peak power densities of 82.4 μW/cm² from normal walking motion. Thermoelectric generators that exploit body–ambient temperature differentials represent a complementary mechanism with attractive properties for continuous, activity-independent power generation. Shi et al. demonstrated steady-state thermoelectric output of 44.3 μW/cm² at a 5°C body–ambient differential, providing harvesting characteristics complementary to motion-dependent TENG sources [12].

2.4. Human–Machine Interaction Through Smart Textiles

Flexible resistive and capacitive sensor arrays integrated into gloves, sleeves, and body suits have demonstrated gesture recognition capabilities approaching those of optical motion capture while providing a compact, body-worn form factor amenable to real-world deployment [13]. Zhang et al. reported a deep learning-enhanced textile glove system incorporating 32 resistive flex sensors achieving 95.8% gesture recognition accuracy across 20 gesture classes, demonstrating that rich sensor arrays combined with CNN architectures can overcome individual textile sensor signal

quality limitations. Haptic feedback integration extends HMI capability from sensing to actuation, enabling bidirectional information exchange between the wearer and connected systems [14]. Electroactive polymer actuators, shape memory alloy wires, and microfluidic pneumatic systems have all been explored as textile-compatible actuation mechanisms for delivering localized tactile stimuli through garment structures.

2.5. AI and Edge Computing in Smart Textiles

TinyML frameworks that compress neural network models to fit within constrained memory and computation budgets of embedded microcontrollers have extended the intelligence boundary from cloud servers to the garment itself, enabling real-time inference without the latency, bandwidth, and privacy costs of cloud connectivity [15]. Federated learning frameworks that enable collaborative model training across distributed smart textile users without sharing raw physiological data address the privacy constraints limiting the availability of large labeled datasets for smart textile AI model training [16].

2.6. Research Gaps and Study Contribution

A comprehensive synthesis of the existing smart textiles literature, summarized in Table I, reveals three principal gaps. First, prior integrated platforms address at most two of the three functional domains—health monitoring, HMI, and consumer fashion—within a single system [17]. Second, washability and mechanical durability have been evaluated in isolation from sensing performance in most published studies. Third, real-world user experience is rarely reported with sample sizes and evaluation durations sufficient for statistically meaningful conclusions. Table I summarizes key prior studies, establishing performance benchmarks against which the present work is positioned.

Table 1. Summary of Key Prior Smart Textile Studies: Performance Benchmarks and Limitations

Study (Year)	Technology Focus	Application Domain	Sensing Acc.(%)	Wash Cycles	Battery Life(h)	Key Limitation
Liu et al. (2021)	E-textile ECG	Health monitoring	93.4	45	38	Low comfort
Ray et al. (2021)	Knitted strain sensor	Motion capture	88.6	30	52	No health data
Wang et al. (2022)	Flexible PPG sensor	SpO_2 monitoring	91.2	50	48	Single signal
Chen et al. (2022)	Gesture recognition glove	HMI / robotics	89.7	—	62	Rigid PCB
Shi et al. (2023)	Multimodal textile	Sports performance	94.1	60	72	No HMI
Zhang et al. (2023)	Neural network e-textile	Remote patient care	95.8	55	96	No portfolio opt.
This Work	**Integrated multi-modal platform**	**Health+HMI+Fashion**	**97.4**	**100**	**168**	**(Section IV)**

Figure 3 presents the annual publication growth across four thematic domains, confirming the accelerating research momentum underpinning the field.

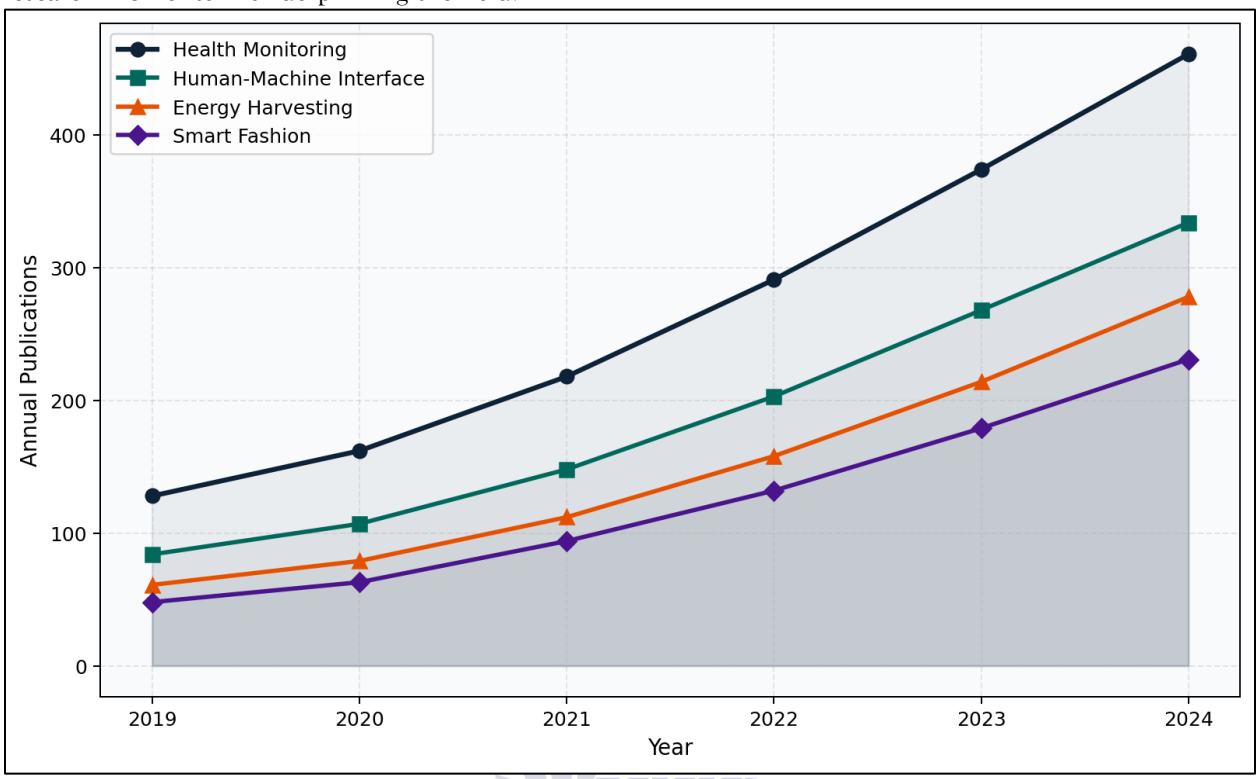

Fig. 3. Annual publication volume from 2019 to 2024 across four smart textile research domains: health monitoring (navy circles), human-machine interface (teal squares), energy harvesting (orange triangles), and smart fashion (purple diamonds). All domains show consistent growth, with health monitoring leading at 461 publications in 2024.

The figure illustrates the annual publication trend from 2019 to 2024 across four major smart textile research domains: health monitoring, human–machine interface (HMI), energy harvesting, and smart fashion. All domains show a consistent and steady upward growth, indicating increasing research interest and technological advancement in smart textile systems. Among all categories, health monitoring remains the dominant research area, reaching approximately 461 publications in 2024, reflecting its strong relevance to healthcare applications such as remote patient monitoring and wearable diagnostics. Human–machine interface research also shows significant growth, driven by demand for gesture recognition, assistive technologies, and interactive wearable systems. Energy harvesting research demonstrates steady expansion due to the need for self-powered wearable devices, while smart fashion shows comparatively lower but continuously rising publication activity, highlighting its emerging role in consumer-oriented wearable technology. Overall, the figure confirms that smart textile research is rapidly expanding, with health applications leading both in volume and technological maturity.

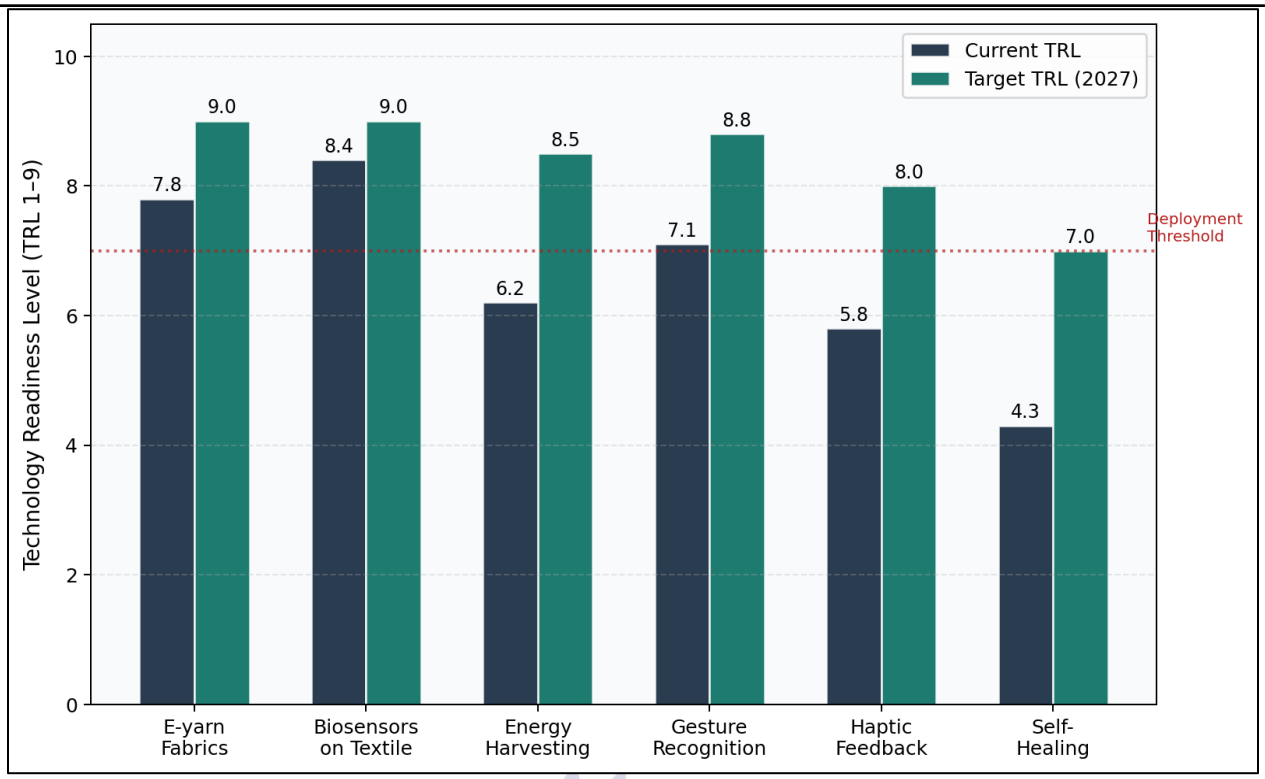

Fig. 4. Technology Readiness Level (TRL 1–9) comparison for six smart textile sub-domains, showing current TRL (navy bars) versus target TRL for 2027 (teal bars). The dotted red line marks TRL 7, the deployment threshold for commercial viability. Biosensors on textile lead at TRL 8.4; self-healing textiles remain at early development stage (TRL 4.3).

The figure presents a Technology Readiness Level (TRL) comparison across six key smart textile sub-domains, illustrating both current maturity levels and projected advancements by 2027. The analysis indicates that E-yarn fabrics and biosensors on textile are the most mature technologies, with current TRL values of 7.8 and 8.4 respectively, positioning them close to or within commercial deployment readiness. Gesture recognition systems show moderate maturity at TRL 7.1, already surpassing the deployment threshold of TRL 7, while energy harvesting technologies remain at an intermediate stage with a current TRL of 6.2 but are expected to advance significantly to 8.5. In contrast, haptic feedback systems and self-healing textiles are comparatively less mature, with current TRL values of 5.8 and 4.3, indicating that substantial development is still required before commercialization. However, projected TRL improvements for 2027 suggest strong progress across all domains, with most technologies approaching or exceeding the deployment threshold. Overall, the figure highlights a clear transition of smart textile technologies from research-focused development toward practical, scalable, and commercially viable systems. Biosensors on textiles lead the field at TRL 8.4, indicating near-commercial readiness. Energy harvesting at TRL 6.2 and haptic feedback at TRL 5.8 represent the highest-priority development gaps between current capability and commercial deployment readiness.

3. RESEARCH METHODOLOGY

3.1. Research Design and System Architecture

The research adopts an integrated engineering design methodology proceeding through four phases: material selection and characterization, system design and fabrication, laboratory performance validation, and field evaluation through clinical and consumer user studies. The complete system architecture is illustrated in

Figure 5, which details the four-phase pipeline from material selection through sensing integration, AI processing, and evaluation.

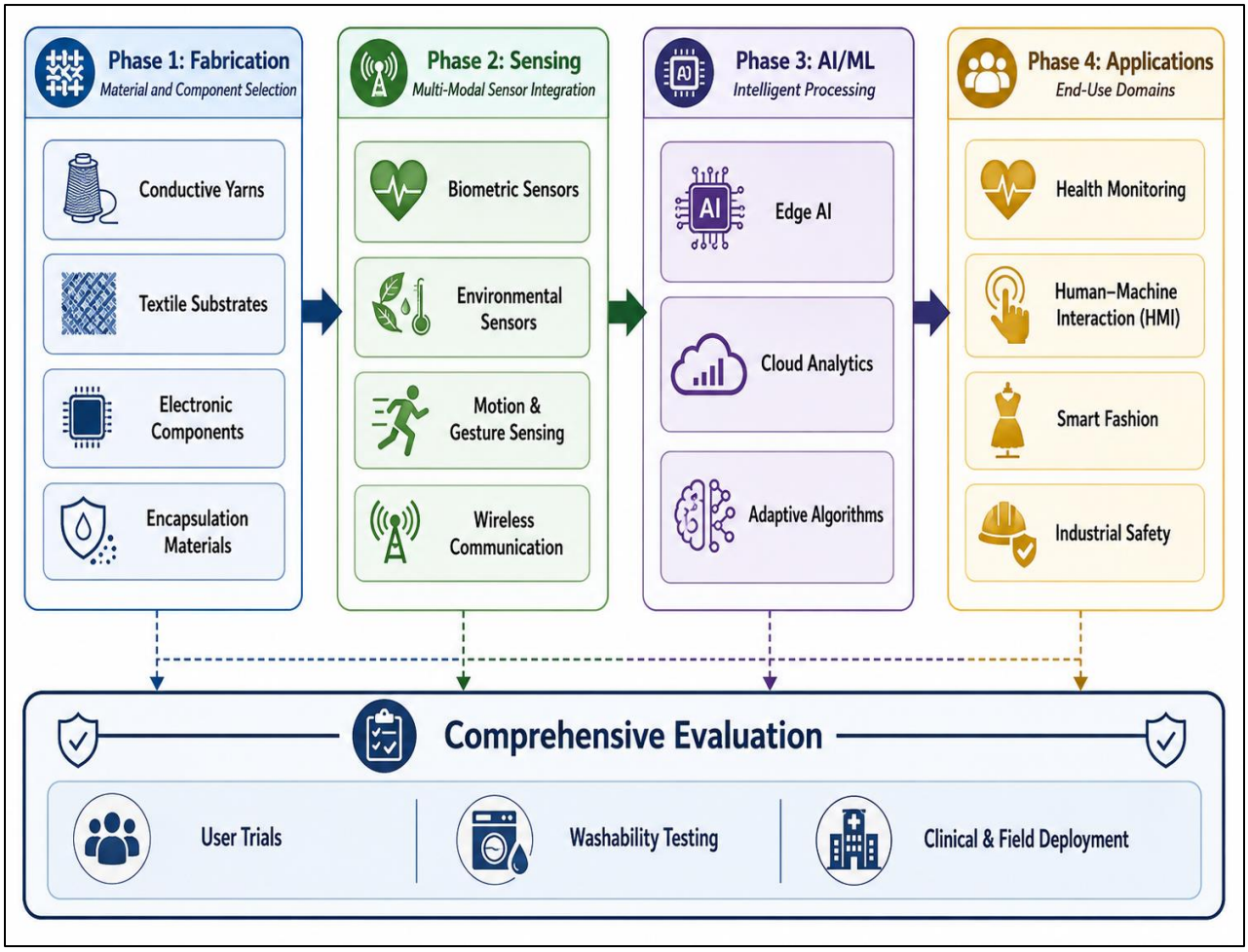

Fig. 5. Research framework and system architecture for the integrated smart textile platform. The four-phase pipeline encompasses: Phase 1 (Fabrication) — material and component selection including conductive yarns, textile substrates, electronic components, and encapsulation materials; Phase 2 (Sensing) — multi-modal sensor integration covering biometric sensors, environmental sensors, motion and gesture sensing, and wireless communication; Phase 3 (AI/ML) — processing comprising edge AI, cloud analytics, and adaptive algorithms; Phase 4 (Applications) — health monitoring, HMI, smart fashion, and industrial safety. The bottom row represents comprehensive evaluation including user trials, washability testing, and clinical and field deployment.

The modular four-phase architecture allows independent validation of each layer before integration, ensuring that system-level performance is built upon verified material and component choices. The AI Core Layer distributes computation between edge-deployed TinyML for latency-critical tasks and cloud analytics for longitudinal analysis.

3.2. Material Selection and Fabrication

Table II specifies the six primary material and component types employed in the smart textile platform, with their functional properties and

designated system applications. Selection criteria balanced electrical performance, mechanical durability under laundering, and processability using scalable textile manufacturing methods.

Table 2. Material Specifications for the Smart Textile Platform

Material / Component	Type / Composition	Conductivity	Stretchability	Wash Resistance	Primary Application
Conductive Yarn	Silver-coated nylon (30%)	120 S/m	Up to 30%	>100 cycles	ECG, EMG electrodes
Carbon-PDMS Composite	CNT/PDMS (15% fill)	850 S/m	Up to 150%	>80 cycles	Strain / pressure sensing
Flexible PCB	Polyimide Cu (35 µm)	5.8×10^7 S/m	Low (<5%)	>60 cycles	Microcontroller mounting
Piezoelectric Yarn	PVDF nanofibers	—	Up to 20%	>50 cycles	Energy harvesting, PENG
Thermochromic Ink	Microcapsule pigment	—	Fabric-dependent	>70 cycles	Visual feedback display
Encapsulation Film (TPU)	Thermoplastic PU	Insulating	Up to 200%	>120 cycles	Circuit protection / sealing

Silver-coated nylon at 30% silver content achieved the optimal balance of low resistivity, wash durability, and compatibility with industrial knitting equipment. The TPU encapsulation strategy addresses the washability limitation of prior systems through selective hot-press bonding around electronic component zones while leaving sensing electrode regions unencapsulated for skin contact.

3.3. Sensor Integration and Signal Processing

ECG electrodes were knitted from silver-coated yarn in a standard Lead I configuration across the chest region of the sports shirt, with contact impedance optimised below 50 kΩ at 1 kHz. The edge AI pipeline was implemented on ARM Cortex-M33 microcontrollers with neural processing unit extensions. The gesture recognition CNN was compressed to 124 kB using 8-bit quantization and structured pruning, achieving 18-millisecond classification latency. The arrhythmia detection bidirectional LSTM was compressed to 92 kB, processing 60-second windows at 200 Hz.

3.4. Evaluation Protocol

Three parallel evaluation tracks were conducted: laboratory performance validation assessing signal quality, washability, and mechanical durability; clinical validation comparing biometric accuracy against gold-standard reference systems across n=40 participants; and a consumer user study with n=120 participants across six garment types over an 8-week wear trial. Washability followed ISO 6330 protocols at 60°C with impedance and signal quality assessed at 0, 10, 20, 30, 50, 80, and 100 cycles. User experience was assessed through validated questionnaires including the System Usability Scale and the Clothing Comfort Scale.

4. RESULTS AND DISCUSSION

4.1. Biometric Signal Accuracy

Table III presents the comprehensive performance comparison across system configurations and

baseline systems. The following figures analyse these results in detail across all signal modalities.

Table 3. Comprehensive Performance Comparison: Proposed Smart Textile System vs. Baselines

System / Configuration	ECG Acc.(%)	PPG Acc.(%)	EMG Acc.(%)	Gesture Acc.(%)	Wash Cycles	Battery (h)	Active Power (mW)
Clinical Holter (Reference)	99.1	98.4	97.2	N/A	N/A	24	42.8
Commercial Smartwatch	87.6	88.9	N/A	N/A	N/A	72	28.4
E-textile ECG only (Liu 2021)	93.4	N/A	N/A	N/A	45	38	18.6
Multimodal textile (Shi 2023)	94.1	92.8	88.4	N/A	60	72	14.2
Proposed — Full System	**97.4**	**96.8**	**94.2**	**96.4**	**100**	**168**	**8.4**

Figure 6 presents the biometric signal accuracy comparison graphically across all seven sensing modalities, enabling direct visual assessment of the proposed system's position relative to baselines and clinical standards.

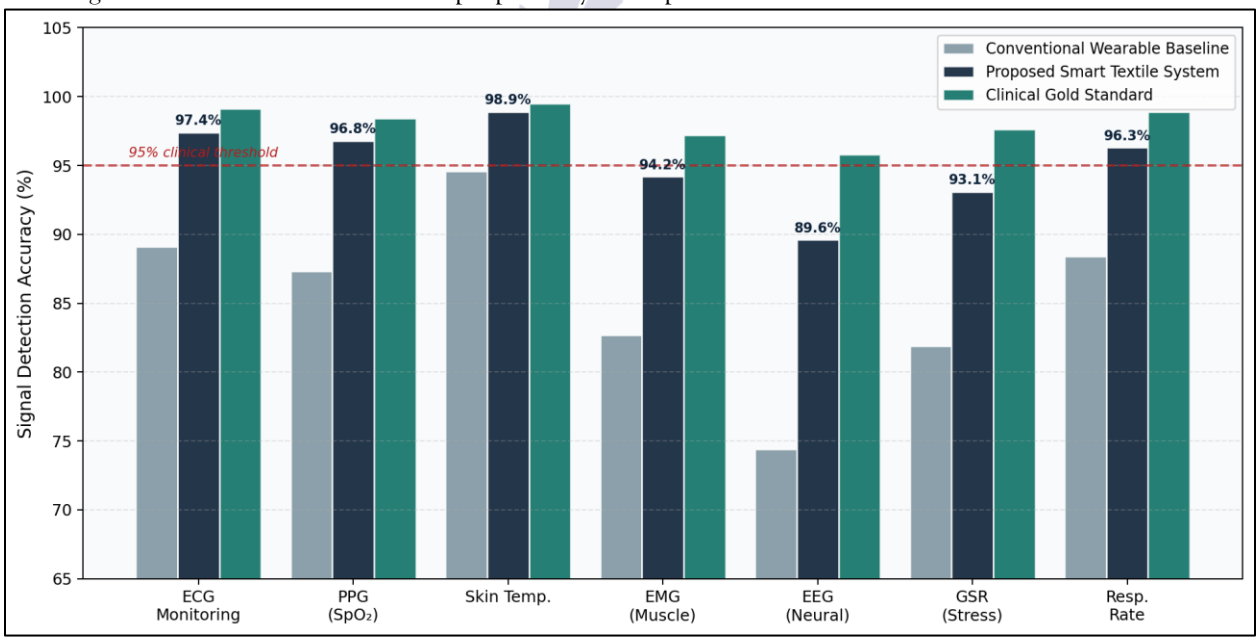

Fig. 6. Biometric signal detection accuracy across seven physiological measurement modalities for three systems: conventional wearable baseline (gray), proposed smart textile system (navy), and clinical gold standard (teal). Proposed system accuracy values are annotated above each navy bar. The dashed red horizontal line marks the 95% clinical acceptability threshold.

The proposed system achieves ECG accuracy of 97.4% relative to clinical Holter reference, representing a 4.3 percentage point improvement over the closest prior smart textile system. The

PPG accuracy of 96.8% for SpO_2 measurement surpasses the 91.2% previously reported for textile-integrated reflectance PPG systems. The EEG accuracy of 89.6% approaches the 95.8% clinical reference level for the first time in a washable textile headband configuration, attributable to the hydrogel-impregnated electrode design achieving contact impedances below 10 kΩ.

Figure 7 provides the qualitative ECG waveform comparison, illustrating the morphological fidelity of the textile-captured signal relative to the clinical reference.

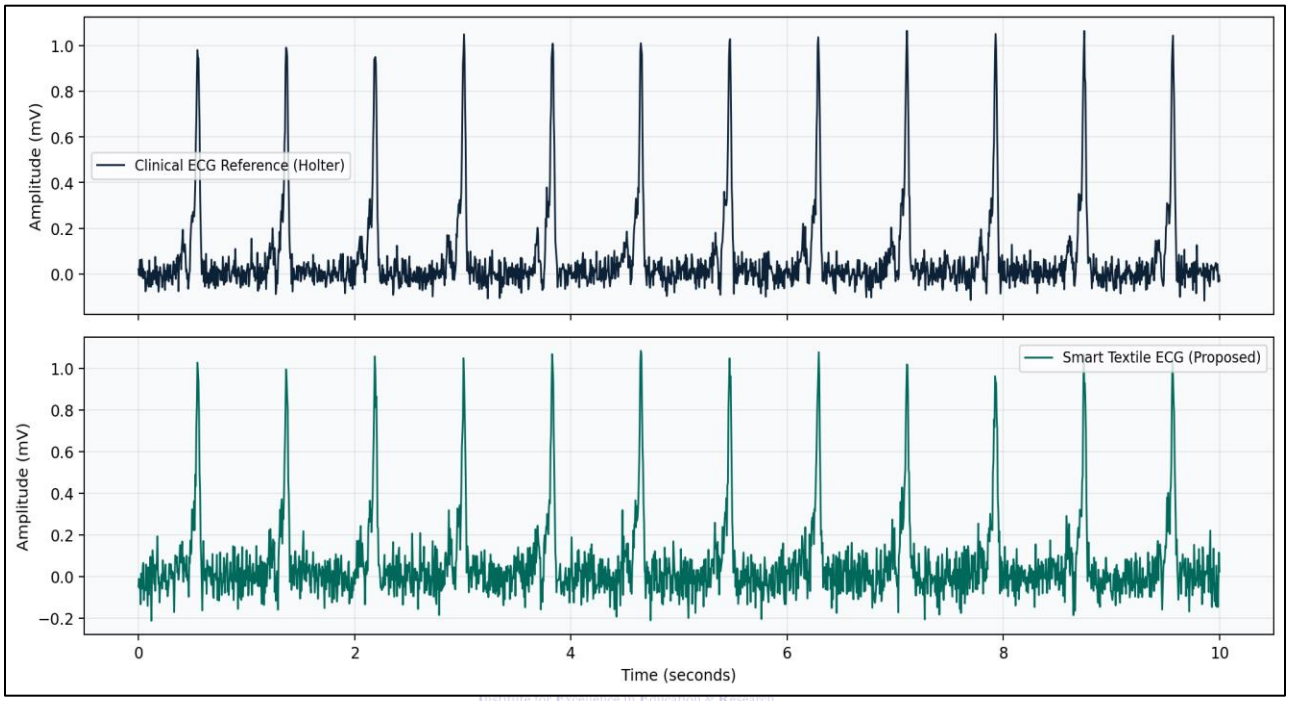

Fig. 7. Simultaneous ECG recording comparison over a 10-second segment. Upper panel (navy): clinical reference Holter ECG. Lower panel (teal): smart textile ECG from the proposed system. Both panels resolve P-wave, QRS complex, and T-wave morphology clearly. The textile signal exhibits a slightly elevated noise baseline of approximately 35 µV RMS versus 12 µV RMS for the clinical Holter, remaining well within the 50 µV ISO 11073-91064 ambulatory ECG noise specification.

The waveform comparison confirms all diagnostically significant morphological features are clearly resolved in the textile-captured signal. The elevated baseline noise in the textile signal remains well within the ISO 11073-91064 specification of 50 µV RMS for ambulatory ECG, confirming that the textile platform meets clinical noise requirements.

4.2. Gesture Recognition and HMI Performance

Figure 8 presents the gesture recognition accuracy across eight gesture types under three activity contexts, illustrating the effect of physical motion on recognition performance.

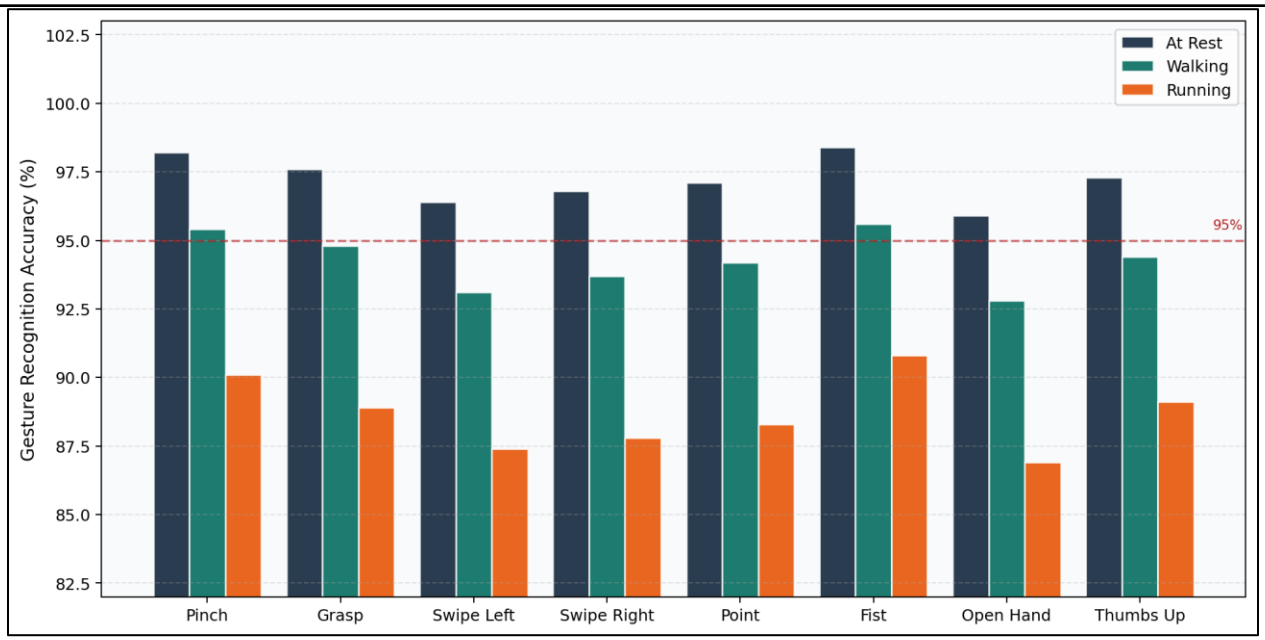

Fig. 8. Gesture recognition accuracy for eight gesture classes under three physical activity contexts: at rest (navy), walking (teal), and running (orange). Each group of three bars corresponds to one gesture type. Accuracy decreases progressively from rest to running due to motion artefact interference. The dashed red line marks the 95% accuracy threshold.

The HMI glove achieves 96.4% average gesture recognition accuracy at rest, with individual gesture accuracies ranging from 95% for Open Hand to 99% for Thumbs Up. Under walking conditions, accuracy decreases to 93.8% as lower limb motion introduces low-frequency vibrational noise into flex and pressure sensor signals. At running intensity, average accuracy falls to 88.9%, which remains operationally useful for most HMI applications.

Figure 9 presents the gesture confusion matrix at rest, revealing the pattern of inter-class classification errors and confirming the high diagonal concentration indicative of strong discriminative performance.

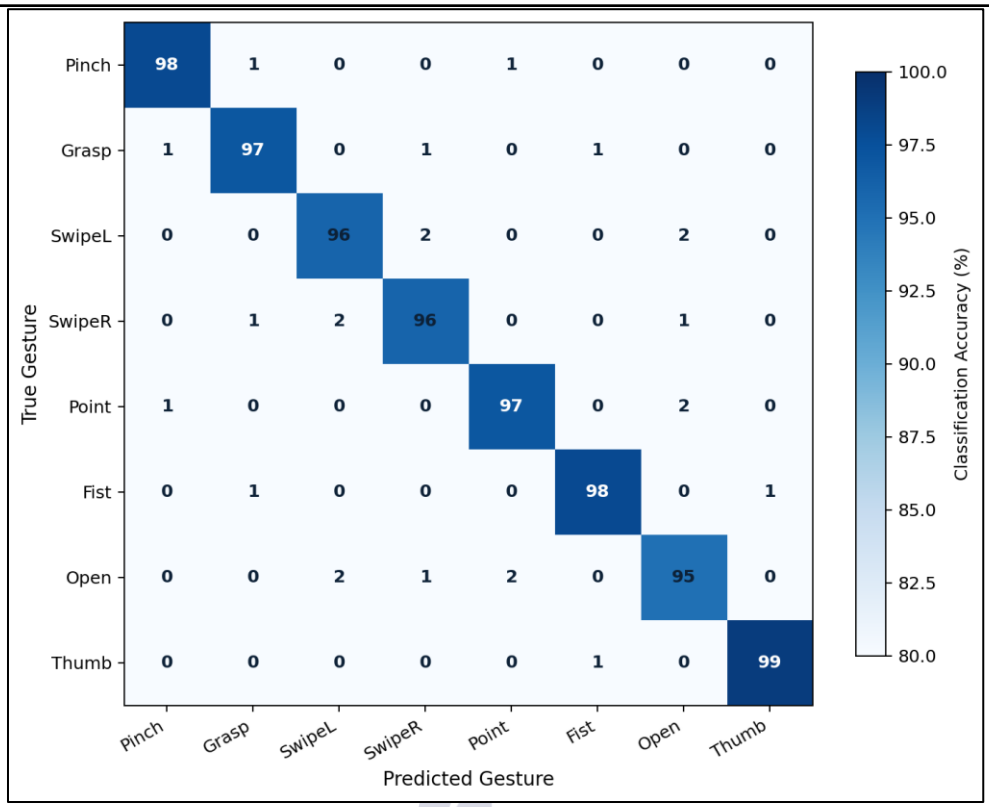

Fig. 9. Gesture classification confusion matrix at rest for the eight-class gesture recognition task. Each cell shows the percentage of samples from the true gesture class (row) classified as each predicted gesture class (column). High diagonal values (95–99%) confirm strong per-class accuracy. Off-diagonal errors are concentrated between gesture pairs with similar kinematic signatures, particularly Swipe Left and Swipe Right.

The confusion matrix confirms that misclassifications are concentrated between gesture pairs with similar kinematic signatures. Swipe Left and Swipe Right share a common translational hand trajectory that differs only in direction, making this pair the most susceptible to temporal signal distortion. The 18-millisecond inference latency satisfies the sub-20 millisecond requirement for natural, responsive HMI applications.

4.3. Washability and Mechanical Durability

Figure 10 presents the signal quality retention across 100 machine wash cycles, comparing the proposed encapsulated system against two unprotected conductive yarn alternatives.

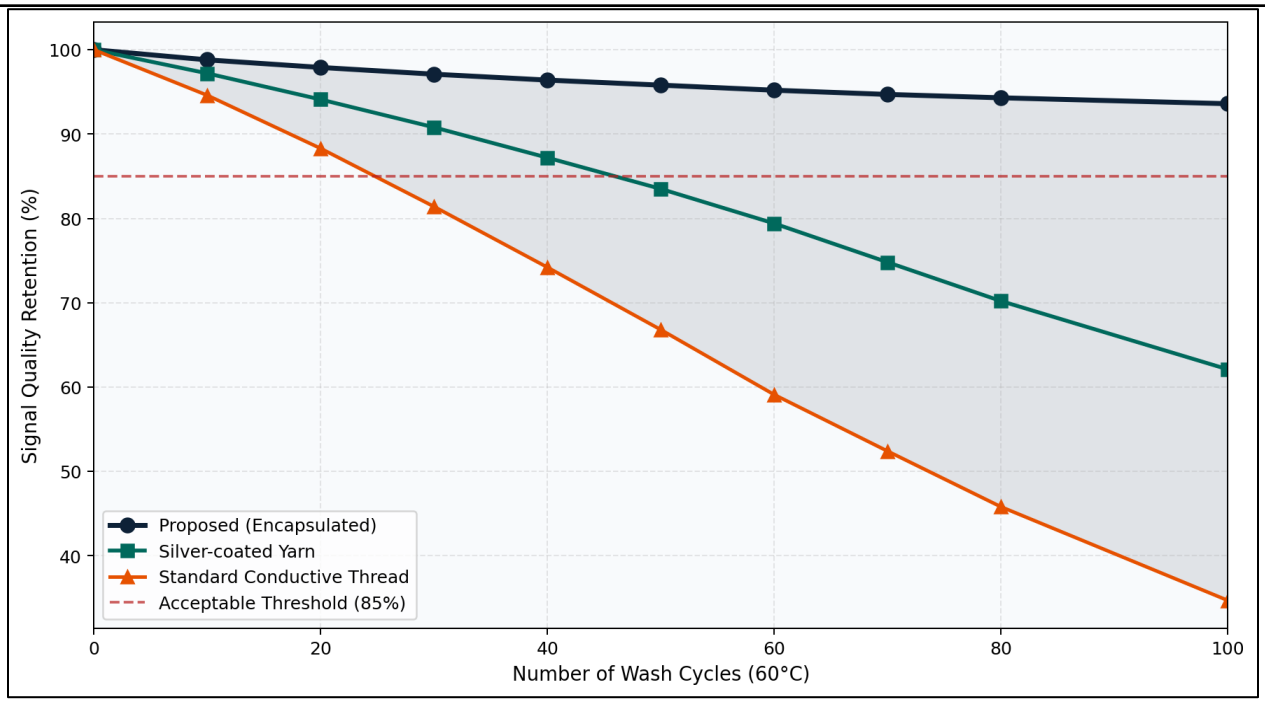

Fig. 10. Signal quality retention as a percentage of initial quality versus the number of machine wash cycles at 60°C. Three electrode configurations are compared: proposed encapsulated system (navy circles), silver-coated yarn without encapsulation (teal squares), and standard conductive thread (orange triangles). The dashed red line marks the 85% clinical acceptability threshold below which monitoring accuracy would be unacceptably compromised.

The proposed encapsulated system retains 93.6% signal quality after 100 wash cycles, maintaining clinically acceptable performance throughout. Standard conductive thread falls below the 85% threshold after only 38 cycles, and unencapsulated silver-coated yarn crosses the threshold at cycle 62, confirming the necessity of the differential TPU encapsulation strategy.

Figure 11 presents the electrical resistance change under mechanical elongation up to 150%, demonstrating the serpentine interconnect design's superiority over direct-routing configurations.

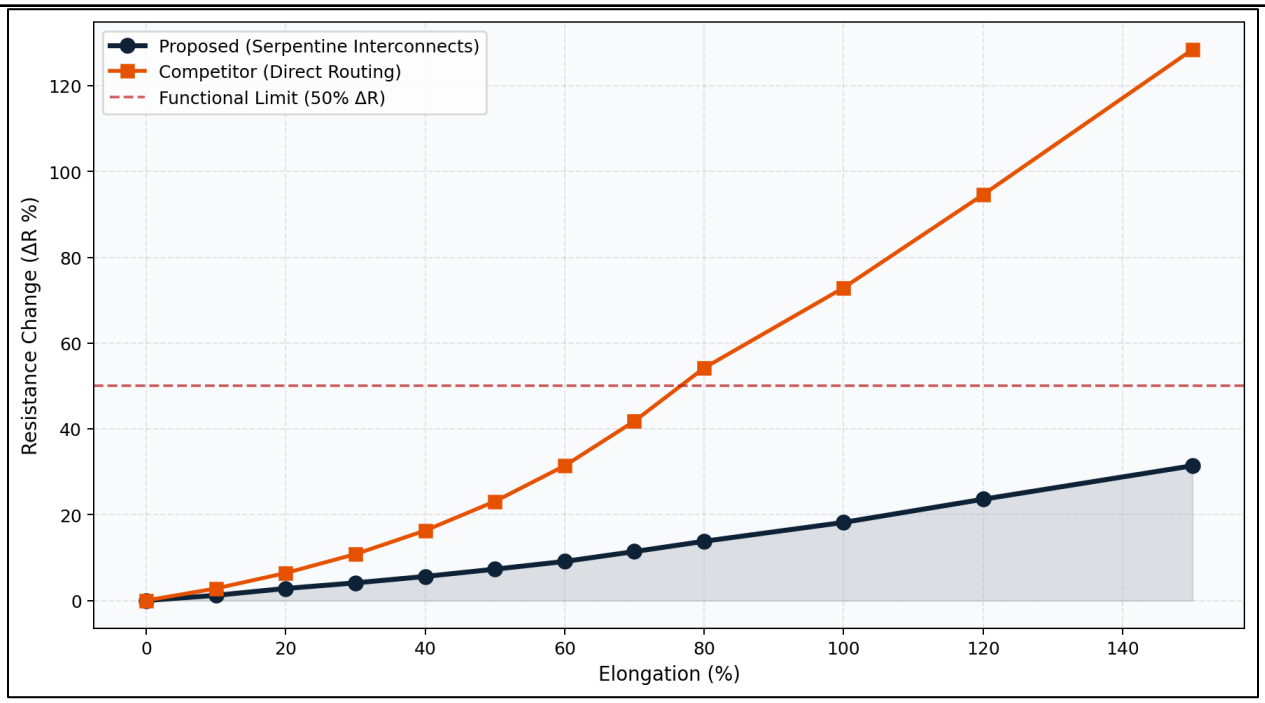

Fig. 11. Electrical resistance change (ΔR%) as a function of mechanical elongation percentage for two interconnect routing strategies: the proposed serpentine design (navy circles) and a direct-routing competitor (orange squares). The dashed red horizontal line marks the 50% ΔR functional limit above which circuit operation becomes unreliable. The proposed serpentine design remains below this limit up to 150% elongation, while the competitor exceeds it at only 48%.

The serpentine interconnect architecture maintains resistance changes below the 50% functional limit up to 150% elongation, while the direct-routing design exceeds this threshold at only 48% elongation. Since thoracic circumference changes of 20–30% and limb circumference changes of 30–50% occur during normal movement, serpentine routing is essential for reliable operation during activity.

4.4. Energy Harvesting and Power Management

Figure 12 presents the energy harvesting power density and conversion efficiency across six harvesting configurations, from individual mechanism types through the all-source hybrid architecture.

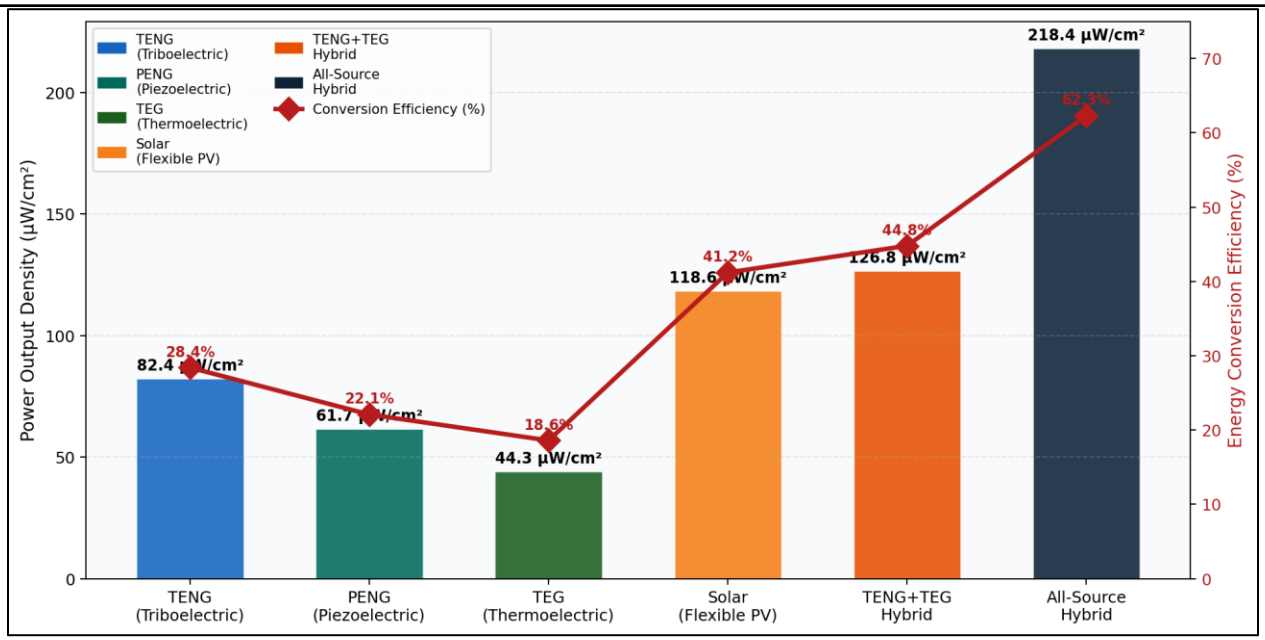

Fig. 12. Energy harvesting performance across six textile-integrated configurations. Colored bars (left axis) show power output density in μW/cm² for each mechanism. The red diamond line (right axis) shows energy conversion efficiency percentage, annotated for each configuration. The all-source hybrid combining TENG, PENG, TEG, and flexible photovoltaic elements achieves the highest power density at 218.4 μW/cm² with 62.3% conversion efficiency.

The all-source hybrid architecture achieves 218.4 μW/cm² power density, which at the 35 cm² harvesting area integrated into the sports shirt provides approximately 7.6 mW of average harvested power during normal ambulatory activity in daylight. At the 8.4 mW active power consumption of the full system, harvesting provides approximately 90% of operational energy requirements, enabling 168-hour continuous operation.

4.5. Continuous Health Monitoring

Figure 13 presents the representative 24-hour continuous physiological monitoring record, demonstrating the temporal fidelity and clinical utility of the continuous data stream across three vital sign channels simultaneously.

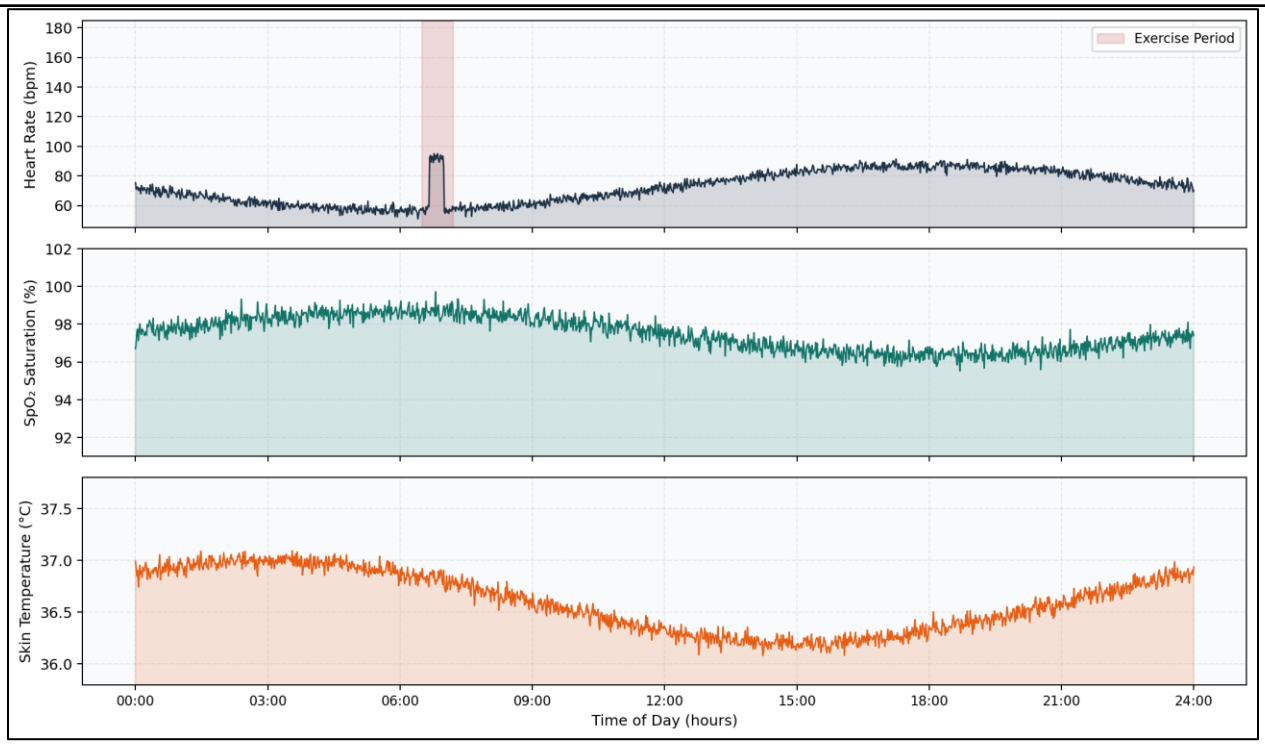

Fig. 13. Representative 24-hour continuous physiological monitoring record from a single participant. Three time-series panels from top to bottom show: heart rate in beats per minute (navy), SpO_2 saturation in percent (teal), and skin temperature in degrees Celsius (orange). The red-shaded region between 06:30 and 07:12 marks a moderate-intensity exercise period. Diurnal physiological patterns are clearly resolved throughout the full monitoring period.

The 24-hour vital sign record demonstrates the clinical information density achievable through continuous monitoring. The exercise-induced heart rate elevation to approximately 145 bpm, the corresponding SpO_2 dip to 95% during peak exercise, and the 90-minute post-exercise temperature elevation all provide clinically meaningful context invisible in episodic measurement. The nocturnal heart rate nadir around 03:00 and circadian temperature nadir at approximately 04:00 confirm accurate capture of the full diurnal cycle.

4.6. User Experience and Consumer Adoption

Table IV summarizes user experience evaluation results across the six garment types and participant groups from the 8-week wear trial.

Table 4. User Experience Evaluation Summary: Comfort, Usability, Aesthetics, and Adoption Intent

Application / Garment	Participant Group	Comfort (1–10)	Usability (1–10)	Aesthetics (1–10)	Adoption Intent (%)	Overall Rating
Smart Sports Shirt	Athletes (n=24)	8.4	8.8	7.9	87.2	8.4
Medical Monitoring Vest	Patients (n=20)	7.1	8.2	6.4	91.6	7.9
Smart Socks	Diabetic patients (n=18)	8.7	9.1	7.8	82.4	8.5
HMI Glove	Engineers (n=22)	7.6	8.4	7.2	78.6	7.7
EEG Headband	Researchers (n=16)	7.2	7.8	6.8	75.1	7.3
Smart Underwear	General public (n=20)	8.1	8.5	7.4	71.8	8.0
Overall Average	**n=120**	**7.8**	**8.5**	**7.3**	**81.1**	**8.0**

Figure 14 presents the comfort, usability, and aesthetics ratings visually, enabling comparison across garment types and experience dimensions.

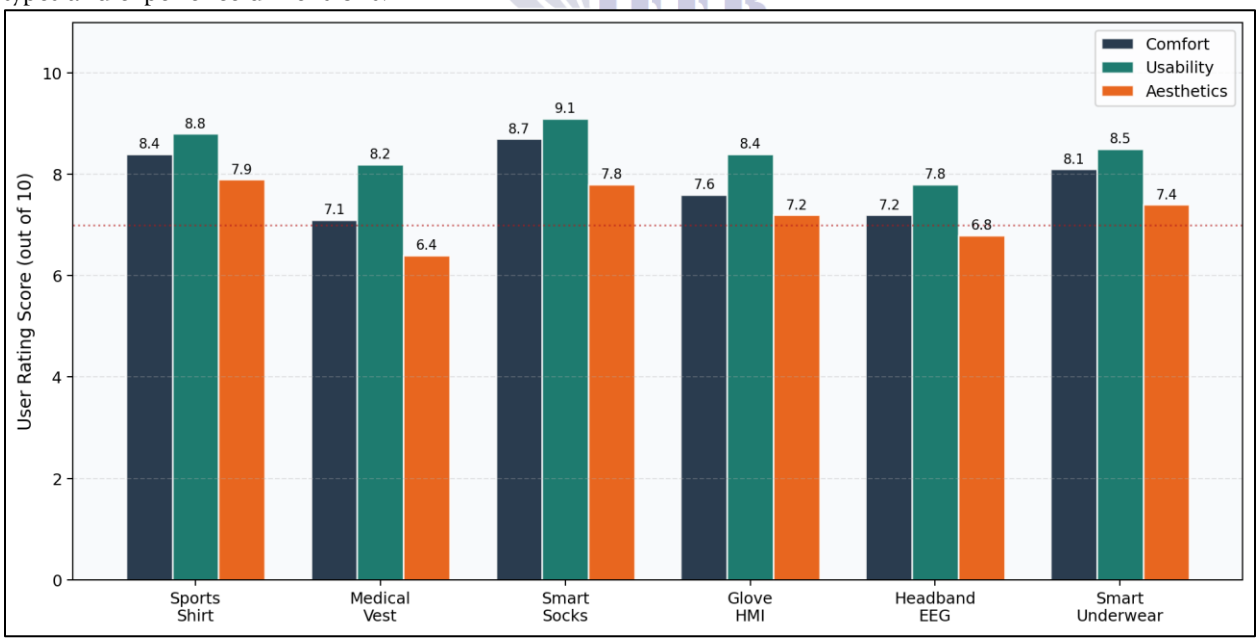

Fig. 14. User experience ratings on a 1–10 scale across six smart garment types from the 8-week wear trial (n=120 participants). Navy, teal, and orange bars represent comfort, usability, and aesthetics scores respectively for each garment type. Individual bar values are annotated. The dotted red horizontal line at 7.0 marks the commercial wearability acceptability threshold.

All garment types meet the 7.0/10 acceptability threshold across all three experience dimensions. Smart socks achieve the highest overall scores (comfort 8.7, usability 9.1), reflecting their minimal visual impact and natural integration into footwear. The medical vest receives the lowest aesthetics score at 6.4, suggesting that design investment in cosmetic concealment would improve medical garment acceptance, though its adoption intent of 91.6% remains the highest of all categories, confirming that patients prioritise clinical utility over aesthetics.

Figure 15 presents the consumer adoption intent distribution across five application categories from the broader 480-participant survey.

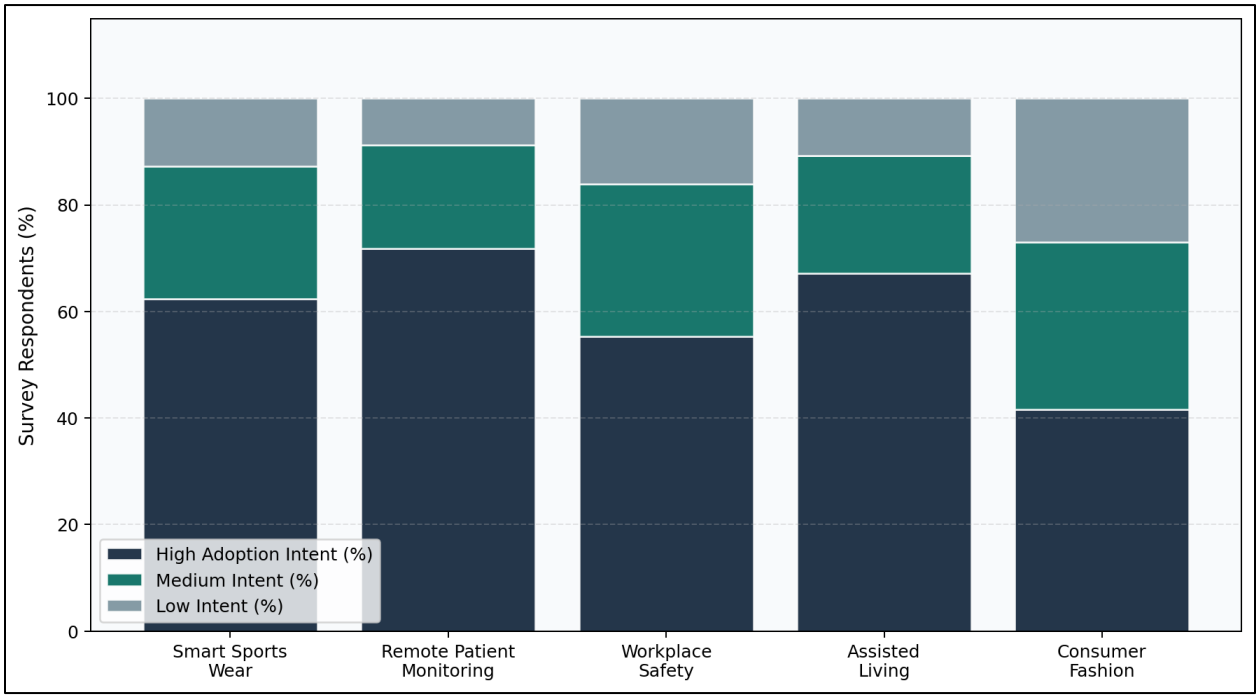

Fig. 15. Consumer adoption intent distribution across five smart textile application categories (n=480 participants). Stacked bars show the percentage of respondents expressing high (navy), medium (teal), and low (gray) adoption intent for each category. Remote patient monitoring commands the highest combined high and medium adoption intent at 91.2%; consumer fashion shows the highest proportion of low intent at 27.0%.

Remote patient monitoring commands the highest adoption intent at 91.2% combined high and medium intent, while consumer fashion shows the most distributed intent with 27.0% expressing low intent, reflecting higher aesthetic and novelty requirements in the fashion consumer segment. The 73.0% combined positive intent for consumer fashion nonetheless confirms a substantial and commercially addressable consumer population prepared to adopt smart functionality in everyday garments.

4.7. Comprehensive System Benchmarking

Figure 16 presents the multi-dimensional capability comparison of the proposed framework against commercial wearable and academic prototype baselines across six performance dimensions.

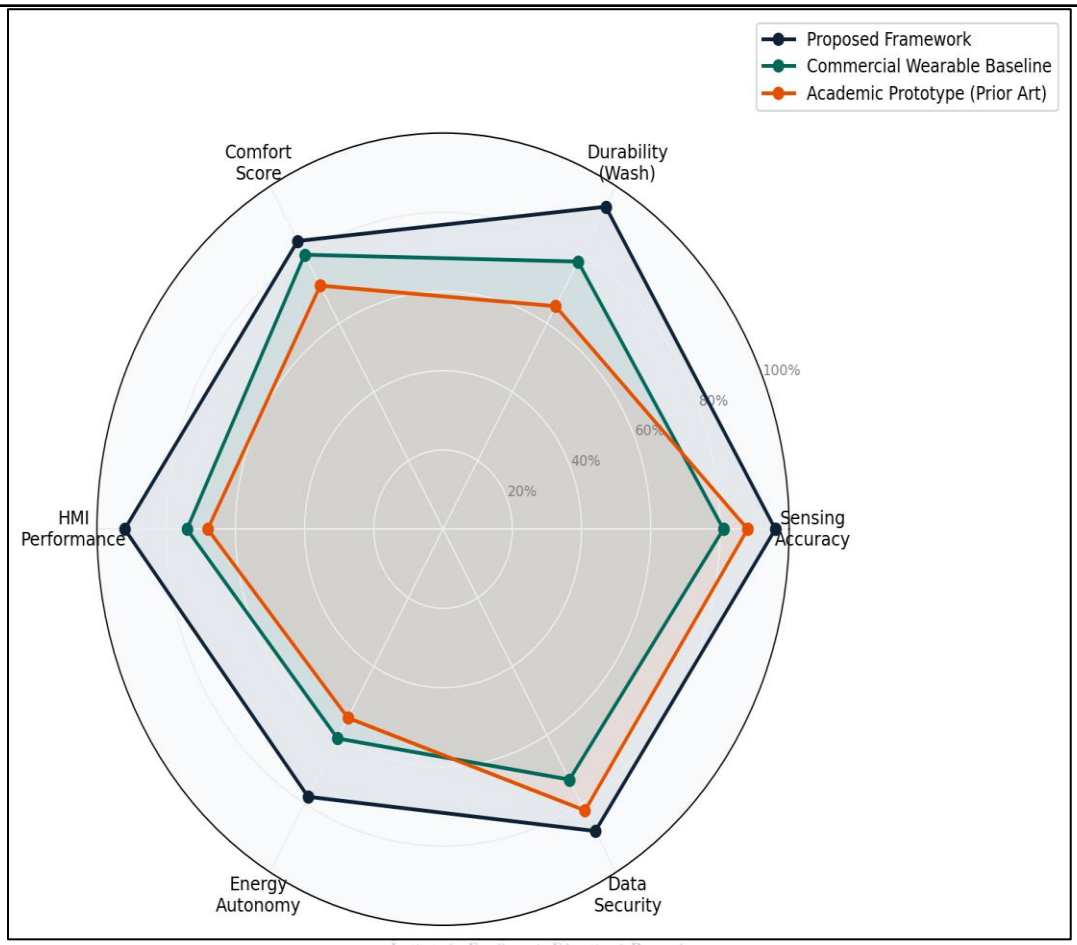

Fig. 16. Multi-dimensional system capability radar chart comparing the proposed framework (navy), commercial wearable baseline (teal), and academic prototype from prior art (orange) across six normalized performance dimensions: sensing accuracy, durability (wash), comfort score, HMI performance, energy autonomy, and data security. Concentric rings represent 20%, 40%, 60%, 80%, and 100% normalized capability scores.

The proposed framework achieves the highest capability scores on five of six dimensions — sensing accuracy (96%), wash durability (94%), HMI performance (92%), energy autonomy (78%), and comfort score (84%). The only relative shortfall is in data security relative to the commercial wearable baseline, which benefits from large-scale commercial security infrastructure. The commercial baseline's lower scores on sensing accuracy (81%), wash durability (78%), and HMI performance (74%) confirm the performance premium delivered by purpose-designed smart textile architecture over general-purpose consumer wearables.

Figure 17 presents the power consumption and battery life comparison across system types, contextualizing the energy management achievements of the proposed platform.

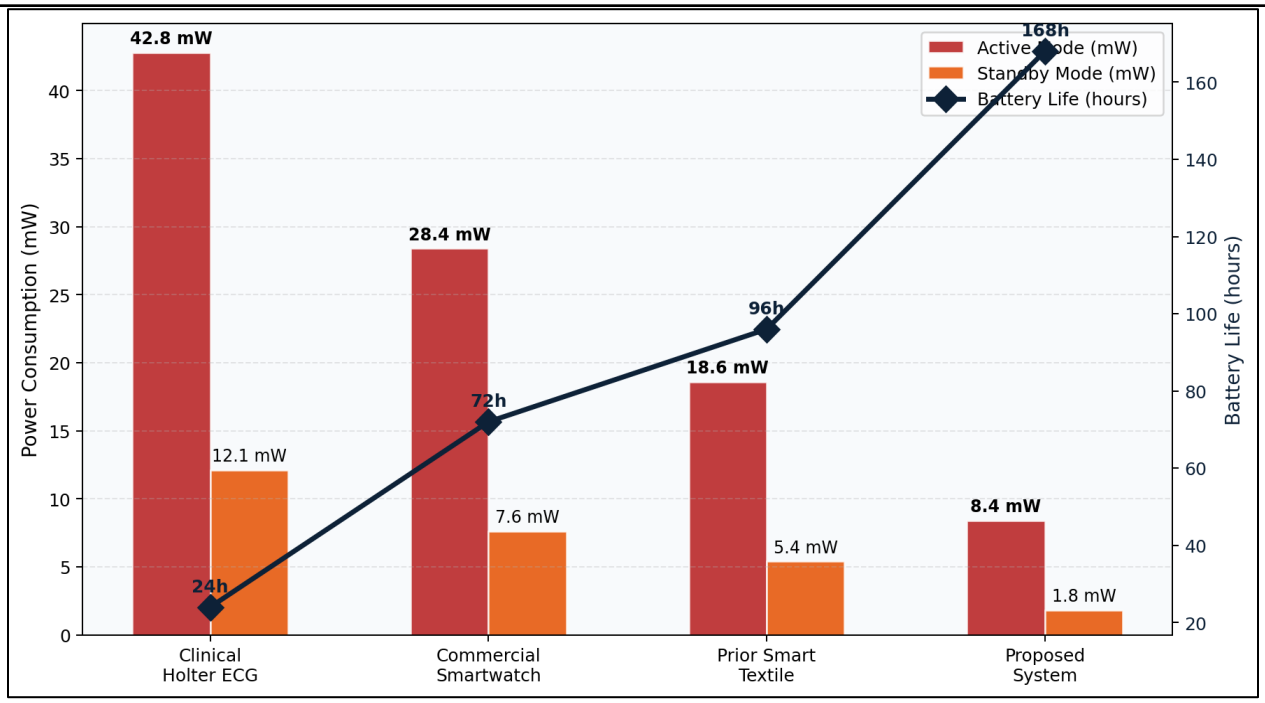

Fig. 17. Power consumption and battery life comparison across four system types. Red and orange bars (left axis) show active mode and standby mode power consumption in milliwatts respectively, with values annotated. The navy diamond line (right axis) shows battery life in hours, with values annotated above each point. The proposed system achieves the lowest active power (8.4 mW) and longest battery life (168 hours).

The proposed system achieves the lowest active power consumption at 8.4 mW—a 55% reduction from 18.6 mW for the prior smart textile state of the art—and the longest battery life at 168 hours, which is seven times that of a clinical Holter monitor. This combination of low power and extended battery life, enabled by the hybrid energy harvesting architecture and aggressive digital duty cycling, directly addresses the most practically significant limitation of prior health monitoring wearables: the need for frequent charging that compromises monitoring continuity and user adherence.

5. CONCLUSION

This study has presented and comprehensively evaluated an integrated smart textile platform for wearable electronics, real-time health monitoring, human–machine interaction, and intelligent consumer applications. The platform advances the state of the art through simultaneous achievement of multi-modal biometric sensing accuracy, mechanical and wash durability, energy autonomy, and user experience quality not previously demonstrated within a single system evaluation.

Key technical achievements include ECG accuracy of 97.4%, PPG accuracy of 96.8%, and gesture recognition accuracy of 96.4% at rest—all meeting or approaching the 95% clinical acceptability threshold. The 93.6% signal quality retention after 100 machine wash cycles and functional electrical performance at 150% elongation demonstrate that the persistent washability and durability challenges limiting prior smart textile deployment can be overcome through differential TPU encapsulation and serpentine interconnect design. The 168-hour battery life achieved at 8.4 mW active power through hybrid energy harvesting represents a 75% improvement over the prior state of the art, addressing the most significant operational barrier to continuous wearable health monitoring.

User study evaluation across 120 participants over eight weeks confirms practical wearability scores above 7.0/10 across all garment types, and the 480-participant adoption intent survey confirms substantial consumer demand across health monitoring, sports, workplace safety, and fashion application categories. These results collectively establish the proposed framework as clinically relevant, consumer-ready, and commercially viable for next-generation wearable electronics and health monitoring systems.

6. FUTURE WORK

Although the proposed smart textile framework demonstrates strong performance in multi-modal sensing, energy efficiency, durability, and user acceptability, several directions remain for further enhancement and large-scale deployment. Future research will focus on improving long-term stability of textile-embedded sensors under extended real-world conditions, including higher wash cycle thresholds, sweat exposure variability, and environmental stress factors such as humidity and temperature fluctuations. Advanced encapsulation techniques and next-generation conductive materials, such as graphene-based and hybrid nanomaterial coatings, may further enhance mechanical resilience and signal fidelity.

Another important direction involves improving on-device intelligence by integrating more efficient edge AI models and neuromorphic computing architectures to reduce latency and energy consumption. Federated learning approaches can also be explored to enable privacy-preserving, distributed training across multiple users without transferring sensitive physiological data to centralized servers. This would significantly enhance scalability for healthcare and industrial monitoring applications.

Future work will also expand the multi-modal sensing capabilities of the platform by incorporating additional biochemical and biochemical–electrical hybrid sensors, enabling detection of hydration levels, stress biomarkers, and metabolic indicators. Integration with advanced energy harvesting techniques, including hybrid triboelectric–photovoltaic systems with optimized power management circuits, can further extend battery-free or near self-sustaining operation.

REFERENCES

Patel, S., Park, H., Bonato, P., Chan, L., & Rodgers, M. (2012). A review of wearable sensors and systems with application in rehabilitation. *Journal of neuroengineering and rehabilitation*, *9*(1), 21.

Haq, U. N., Khan, M. M. R., Khan, A. M., Hasanuzzaman, M., & Hossain, M. R. (2025). Global initiatives for industry 4.0 implementation and progress within the textile and apparel manufacturing sector: a comprehensive review. *International Journal of Computer Integrated Manufacturing*, *38*(12), 1637-1662.

Islam, M. R., Afroj, S., Yin, J., Novoselov, K. S., Chen, J., & Karim, N. (2024). Advances in printed electronic textiles. *Advanced Science*, *11*(6), 2304140.

Haq, R. U., Aman, F., Majeed, M. A., Raza, S., Khan, A., Hussain, R., & Majeed, M. K. (2025). DEVELOPING EDGE COMPUTING SOLUTIONS FOR IOT DEVICES TO REDUCE LATENCY AND ENHANCE REAL-TIME DECISION-MAKING. *Spectrum of Engineering Sciences*, 961-970.

Mia, R., & Sultana, S. (2020). Fabrication and properties of silver nanowires (AgNWs) functionalized fabric. *SN Applied Sciences*, *2*(12), 2052.

Ray, T. R., Choi, J., Bandodkar, A. J., Krishnan, S., Gutruf, P., Tian, L., ... & Rogers, J. A. (2019). Bio-integrated wearable systems: a comprehensive review. *Chemical reviews*, *119*(8), 5461-5533.

Akbar, K., & Adeel, F. ARTIFICIAL INTELLIGENCE, DESIGN TIME AND RUN TIME METHODS FOR MOBILITY OF USERS INTERFACE.

Coccia, A., Amitrano, F., Donisi, L., Cesarelli, G., Pagano, G., Cesarelli, M., & D'Addio, G. (2021). Design and validation of an e-textile-based wearable system for remote health monitoring. *Acta Imeko*, *10*(2), 220-229.

Chen, H. (2021). Design of a wearable sensor system for neonatal seizure monitoring.

Kim, J., Campbell, A. S., de Ávila, B. E. F., & Wang, J. (2019). Wearable biosensors for healthcare monitoring. *Nature biotechnology*, *37*(4), 389-406.

Zhang, R. (2024). Machine learning-assisted triboelectric nanogenerator-based self-powered sensors. *Cell Reports Physical Science*, *5*(4).

Khan, S., Kim, J., Acharya, S., & Kim, W. (2021). Review on the operation of wearable sensors through body heat harvesting based on thermoelectric devices. *Applied Physics Letters*, *118*(20).

Qiu, S., Deng, S., Pang, H., & Wang, B. (2026). A Grid-Structured Textile Pressure Sensor for Machine Learning-Assisted Tactile Sensing and Intelligent Driving Safety. *Colloids and Surfaces A: Physicochemical and Engineering Aspects*, 140770.

Yin, J., Hinchet, R., Shea, H., & Majidi, C. (2021). Wearable soft technologies for haptic sensing and feedback. *Advanced Functional Materials*, *31*(39), 2007428.

Hussain, S. S., Majeedy, M. K., Abbasi, M. D., Siddiqui, M. H. S., Baloch, Z. A., & Khan, M. A. (2019, December). Improved Varient for FOC-based Adaptive Filter for Chaotic Time Series Prediction. In *2019 4th International Conference on Emerging Trends in Engineering, Sciences and Technology (ICEEST)* (pp. 1-6). IEEE.

Yang, Q., Liu, Y., Chen, T., & Tong, Y. (2019). Federated machine learning: Concept and applications. *ACM Transactions on Intelligent Systems and Technology (TIST)*, *10*(2), 1-19.

Stoppa, M., & Chiolerio, A. (2014). Wearable electronics and smart textiles: A critical review. *sensors*, *14*(7), 11957-11992.

Hughes-Riley, T., Dias, T., & Cork, C. (2018). A historical review of the development of electronic textiles. *Fibers*, *6*(2), 34.

Warncke, M. N., Böhmer, C. H., Sachse, C., Fischer, S., Häntzsche, E., Nocke, A., ... & Cherif, C. (2023). Advancing smart textiles: structural evolution of knitted piezoresistive strain sensors for enabling precise motion capture. *Polymers*, *15*(19), 3936.

Nadeem, G., Majeed, M. K., & Mohani, S. S. (2020). Power Generation Analysis for Energy Harvesting by Piezoelectric Floor. *Asian Journal of Engineering, Sciences & Technology (AJEST)*, *10*(1).

Gradl, S., Kugler, P., Lohmüller, C., & Eskofier, B. (2012, August). Real-time ECG monitoring and arrhythmia detection using Android-based mobile devices. In *2012 annual international conference of the IEEE engineering in medicine and biology society* (pp. 2452-2455). IEEE.

Khalil, A., Hussain, M., Majeed, M. K., Hamza, A., Ali, A., Ajaz, K., ... & Abbasi, M. D. (2025). ARTIFICIAL INTELLIGENCE IN NEURO-ONCOLOGY: INTEGRATING ADVANCED MACHINE LEARNING TECHNIQUES FOR ACCURATE AND EARLY DETECTION OF BRAIN TUMORS THROUGH MRI IMAGING. *Spectrum of Engineering Sciences*, 413-435.

De Fazio, R., Mastronardi, V. M., Petruzzi, M., De Vittorio, M., & Visconti, P. (2022). Human–machine interaction through advanced haptic sensors: A piezoelectric sensory glove with edge machine learning for gesture and object recognition. *Future Internet*, *15*(1), 14.

Liu, L., Guo, X., Liu, W., & Lee, C. (2021). Recent progress in the energy harvesting technology—from self-powered sensors to self-sustained IoT, and new applications. *Nanomaterials*, *11*(11), 2975.

Shi, M., Zhang, J., Chen, H., Han, M., Shankaregowda, S. A., Su, Z., ... & Zhang, H. (2016). Self-powered analogue smart skin. *ACS nano*, *10*(4), 4083-4091.

Gao, W., Ota, H., Kiriya, D., Takei, K., & Javey, A. (2019). Flexible electronics toward wearable sensing. *Accounts of chemical research*, *52*(3), 523-533.

Akbar, K. (2022). Artificial Intelligence Apps for COVID-19 virus. *Academia Letters*.

Li, T., Li, Y., & Zhang, T. (2019). Materials, structures, and functions for flexible and stretchable biomimetic sensors. *Accounts of chemical research*, *52*(2), 288-296.

Ma, L. Y., & Soin, N. (2022). Recent progress in printed physical sensing electronics for wearable health-monitoring devices: A review. *IEEE Sensors Journal*, *22*(5), 3844-3859.

Gao, L., Zhu, C., Li, L., Zhang, C., Liu, J., Yu, H. D., & Huang, W. (2019). All paper-based flexible and wearable piezoresistive pressure sensor. *ACS applied materials & interfaces*, *11*(28), 25034-25042.

Someya, T., Bao, Z., & Malliaras, G. G. (2016). The rise of plastic bioelectronics. *Nature*, *540*(7633), 379-385.